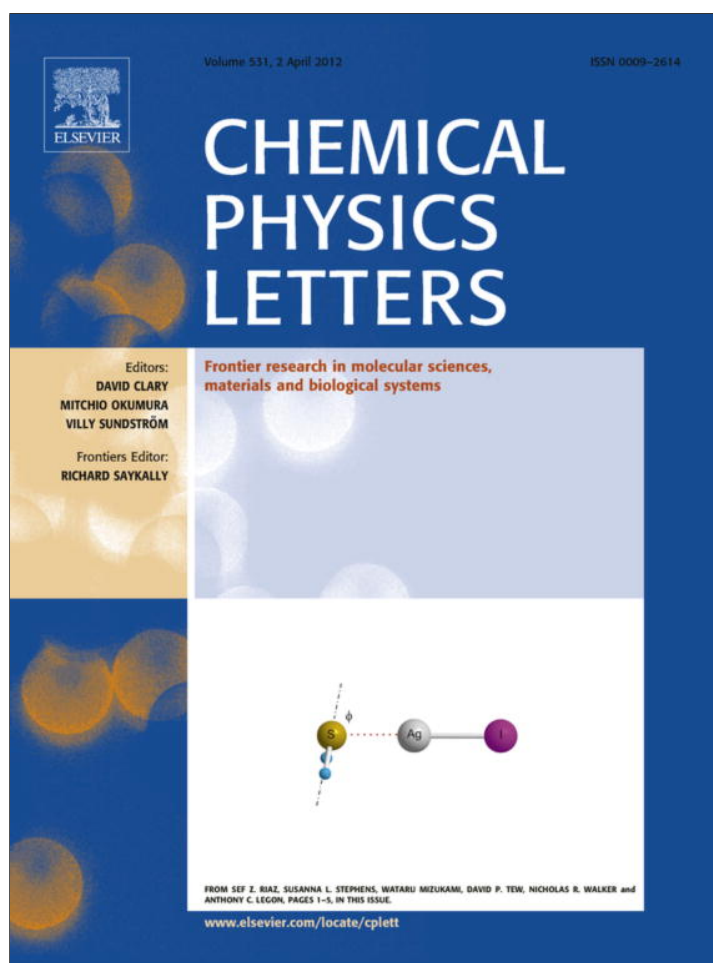


Provided for non-commercial research and education use.  
Not for reproduction, distribution or commercial use.



This article appeared in a journal published by Elsevier. The attached copy is furnished to the author for internal non-commercial research and education use, including for instruction at the authors institution and sharing with colleagues.

Other uses, including reproduction and distribution, or selling or licensing copies, or posting to personal, institutional or third party websites are prohibited.

In most cases authors are permitted to post their version of the article (e.g. in Word or Tex form) to their personal website or institutional repository. Authors requiring further information regarding Elsevier's archiving and manuscript policies are encouraged to visit:

<http://www.elsevier.com/copyright>



Contents lists available at SciVerse ScienceDirect

## Chemical Physics Letters

journal homepage: [www.elsevier.com/locate/cplett](http://www.elsevier.com/locate/cplett)

## Multinuclear NMR relaxometry studies in singly fluorinated liquid crystal

M. Rajeswari<sup>a,\*</sup>, Trivikram R. Molugu<sup>a,b</sup>, S. Dhara<sup>a</sup>, K. Venu<sup>c</sup>, V.S.S. Sastry<sup>a</sup>, R. Dabrowski<sup>d</sup><sup>a</sup> School of Physics, University of Hyderabad, Hyderabad 500 046, India<sup>b</sup> Department of Chemistry, University of Arizona, Tucson, AZ 85721, USA<sup>c</sup> Soctronics Technologies Pvt. Ltd., Banjara Hills, Hyderabad 500 034, India<sup>d</sup> Institute of Chemistry, Military University of Technology, 00-908 Warsaw, Poland

## ARTICLE INFO

## Article history:

Received 26 September 2011

In final form 6 February 2012

Available online 15 February 2012

## ABSTRACT

Nuclear spin–lattice relaxation rate dispersion study of <sup>1</sup>H and <sup>19</sup>F in the isotropic phase of a singly fluorinated liquid crystal 4'-butoxy-3-fluoro-4-isothiocyantotolane (4OTOLFo) points to their differing relaxation pathways and hence sensitivity to qualitatively different time modulations. In particular fluorine nuclear spins, with strong lattice coupling (larger by two orders) extending to very low frequencies, detect slowly relaxing local structures via the spin–rotation interaction. The field-cycling technique used to carry out these very low frequency measurements, provides for level crossing of the two nuclear species at low enough jump fields, facilitating an additional mechanism of cross-relaxation in the strong coupling limit.

© 2012 Elsevier B.V. All rights reserved.

## 1. Introduction

NMR spectroscopy and relaxometry are powerful and well established experimental techniques to study orientational order and molecular dynamic processes in liquid crystalline systems [1–3]. In particular, relaxometry is rather unique to investigate slow collective motions that usually occur in such soft systems over a dynamic range spanning from tens of kHz to hundreds of MHz [4,5]. In the present study we have chosen a fluorinated liquid crystal (with a lone fluorine on its aromatic core), which has two spin  $\frac{1}{2}$  nuclei (<sup>1</sup>H and <sup>19</sup>F) having only slightly differing gyromagnetic ratios, with the objective of comparing the underlying processes reported by these two species through their spin–lattice relaxation profiles. In general the proton spin–lattice relaxation (in the wide-line NMR regime of interest here) is essentially mediated by inter-nuclear dipole interaction, and hence sensitive to reorientational time correlations. Its interpretation has been well established in terms of various dynamic processes in the liquid crystal systems. However relaxation pathways of lone fluorine could be in principle several: e.g., inter-molecular dipolar interaction with other fluorine nuclei; hetero-nuclear dipolar interaction with protons; effects due to chemical shift anisotropy (CSA) and spin–rotation interaction (SR). The first mechanism, mediated by translational diffusion, is too fast to display dispersion in the frequency range of our study, while the second should lead to dispersions similar to protons. The experimental data indicating strong coupling of fluorines to the bath, relative to protons however suggest that there are other more effective pathways of relaxation. CSA

mechanism, important at the usual laboratory frequencies ( $\sim 10^2$  MHz), is negligible in a field-cycling experiment focussed on sub-MHz regime, owing to its field dependence. We find that the main contribution to fluorine spin–lattice relaxation rate ( $R_1$ ) here is from spin–rotation interaction modulated by torques on the molecule and hence sensitive to angular momentum time correlations. In contrast, the protons are sensitive, via dipolar interactions, to molecular reorientational time correlations. Such fluorinated compounds have attracted recently significant attention because of their applications in liquid crystal display technology and telecommunications [6–14]. Extensive optical and dielectric measurements were carried out on these systems to study their electro-optical and physical properties [11,12]. The present study reports contrasting relaxation rate dispersions of proton and fluorine nuclei as a function of Larmor frequency in the liquid crystal 4'-butoxy-3-fluoro-4-isothiocyantotolane (4OTOLFo) in its isotropic phase at different temperatures.

The present Letter is organized as follows. In Section 2 we discuss the experimental details and present results on  $R_1$  as a function of frequency and temperature. In the next section, we discuss relaxation mechanisms for proton and fluorine, and present models which provide quantitative estimates of their contributions. Section 4 discuss the analysis of our findings in terms of relevant dynamic models, while salient features are summarized in the concluding section.

## 2. Experimental details

This compound was synthesized and its phase sequence was determined in the laboratories of Warsaw [15,16], and these are presented in Figure 1. For our experiment, the compound was

\* Corresponding author.

E-mail address: [raji.hcu@gmail.com](mailto:raji.hcu@gmail.com) (M. Rajeswari).

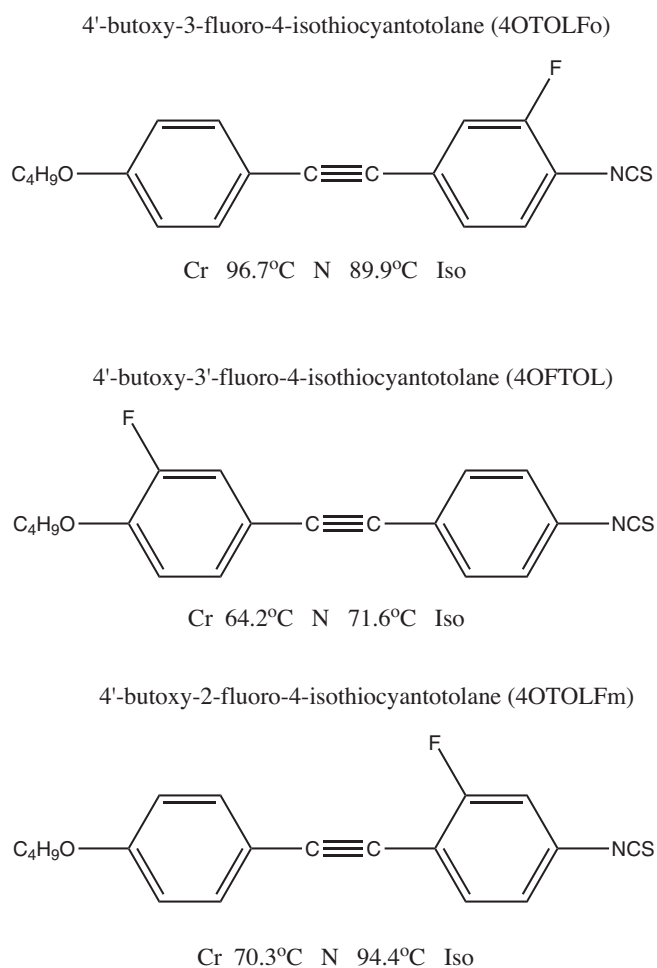


**Figure 1.** Molecular structure and phase sequence of a liquid crystal 4OTOLFo (molecular structures of other related fluorine compounds are also given for comparison).

sealed in an NMR tube under vacuum after removing the dissolved oxygen by freeze–pump–thaw technique. Frequency dispersions of  $R_1$  were recorded with two spectrometers. A Fast Field Cycling NMR relaxometer (SPINMASTER FFC-2000, Stellar) was used to cover the low frequency range (10 kHz to 10 MHz), and the higher frequency data were collected with a home-built variable-field pulsed NMR spectrometer (extending to 50 MHz). A prepolarized pulse sequence was used for all field-cycling measurements below 4 MHz, while a non-prepolarized pulse sequence was used above 4 MHz. The prepolarized and acquisition frequencies were 10 and 9.25 MHz, respectively. Typical switching time during the field cycle is 3 ms, and the duration of the  $\pi/2$  pulse is 6  $\mu$ s. Other parameters were optimized catering specifically to each spin system. An inversion recovery pulse sequence with a  $\pi/2$  pulse width of 4.5  $\mu$ s was used at higher frequencies (20–50 MHz) on the home-built spectrometer. The temperature ( $T$ ) of the sample was controlled (to within 0.1 °C) by passing thermostated dry air over the sample. The frequency dispersion profiles of proton and fluorine thus obtained at different temperatures in the isotropic phase are shown in Figures 2–4. The temperature dependences of the relaxation rates were also measured at chosen Larmor frequencies  $\nu_L$  ( $\omega = 2\pi\nu_L$ ), and are shown in Figure 5. The experimental errors involved in the measurements on proton were estimated to be less than 2%, while those on fluorine were about 5% due to poor signal strength. The  $R_1$  dispersion profiles of proton show frequency independence in the sub-MHz region, and onset of moderate dispersions at higher frequencies as the sample is cooled

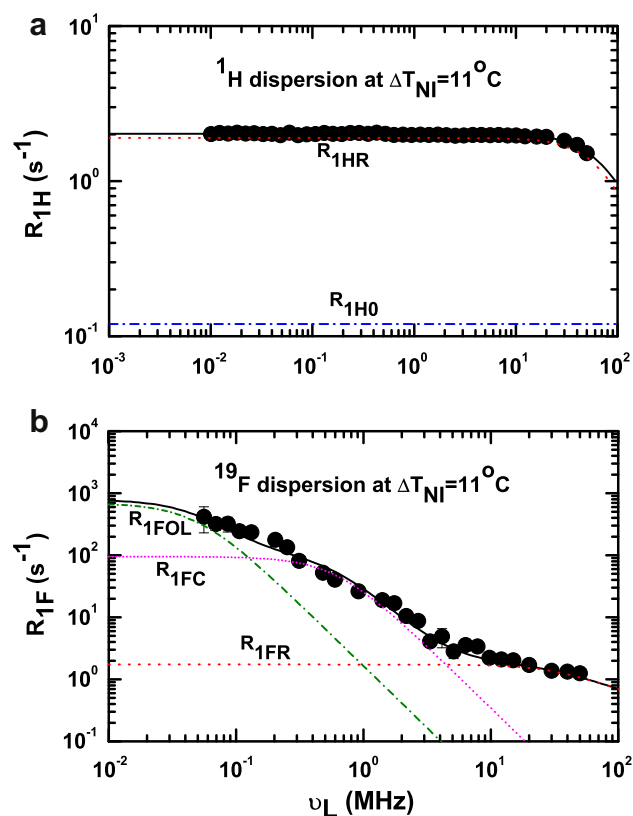


**Figure 2.** Proton (a) and fluorine (b) spin–lattice relaxation rate dispersions fitted to Eqs. (3) and (8) at  $\Delta T_{NI} = 11$  °C. The color dotted lines represents the contribution from different molecular processes. (For interpretation of the references to color in this figure legend, the reader is referred to the web version of this article.)

towards the isotropic-to-nematic transition temperature ( $T_{NI}$ ). The fluorine dispersion data on the other hand show a contrasting behavior. They all exhibit a significant dispersion even at the lowest of the frequencies irrespective of the temperature of the sample, signaling the presence of strong and highly dispersive fluorine coupling to the lattice. The temperature dependent fluorine relaxation rate measurements at different Larmor frequencies (Figure 5) also support this observation. The interpretation of fluorine data thus should focus on identifying plausible mechanism(s) exclusively sensitive to low frequency microscopic dynamics, but could not be reported by protons.

### 3. Relaxation models

In this section, we present dynamic models relevant for the analysis of the observed proton and fluorine dispersions. Underlying molecular mechanisms mediating nuclear spin relaxation processes in liquid crystals have been comprehensively reviewed earlier [1–3,17], and interpretation of dispersions of proton data (wide-line NMR regime) is based on them [1]. The stronger lattice-coupling of fluorine (a magnetically comparable spin  $\frac{1}{2}$  nucleus residing on the same molecule) extending to even very low fields points to the important role of its relatively larger spin–rotation interaction in providing an efficient relaxation pathway, and analysis of its dispersion explores possible slow dynamic processes modulating SR interaction.

#### 3.1. Proton relaxation

Proton spin–lattice relaxation, via the dipole–dipole interactions of spin pairs, is influenced by time modulations due to:

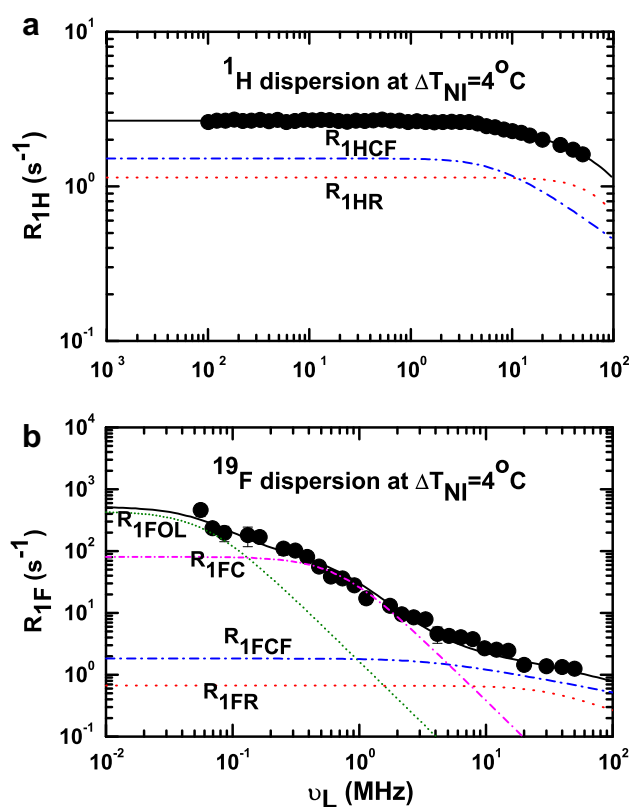


**Figure 3.** Proton (a) and fluorine (b) spin–lattice relaxation rate dispersions fitted to Eqs. (3) and (8) at  $\Delta T_{NI} = 4$  °C. The color dotted lines represents the contribution from different molecular processes. (For interpretation of the references to color in this figure legend, the reader is referred to the web version of this article.)

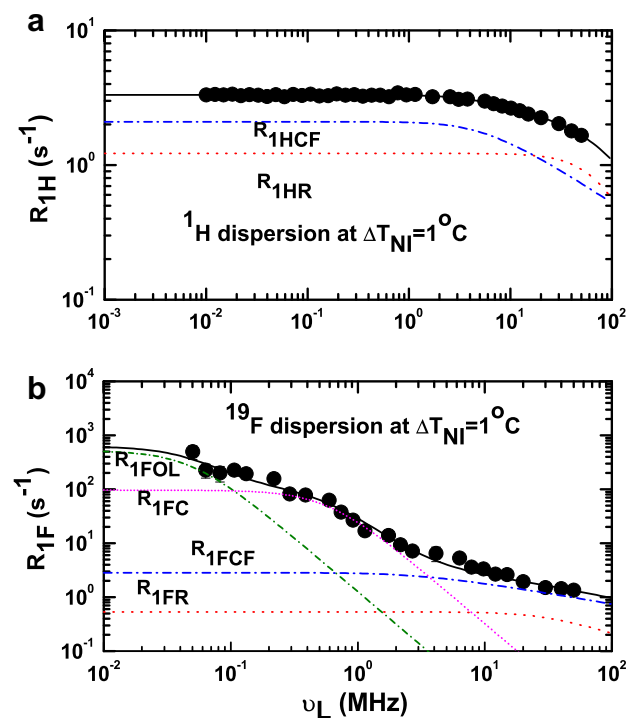


**Figure 4.** Proton (a) and fluorine (b) spin–lattice relaxation rate dispersions fitted to Eqs. (3) and (8) at  $\Delta T_{NI} = 1$  °C. The color dotted lines represents the contribution from different molecular processes. (For interpretation of the references to color in this figure legend, the reader is referred to the web version of this article.)

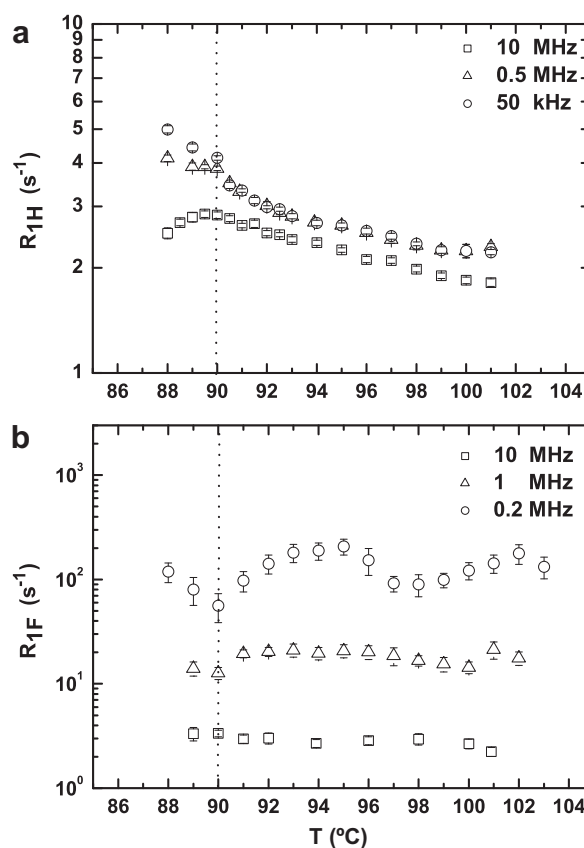


**Figure 5.** Temperature dependence of spin–lattice relaxation rates plotted against temperature at different Larmor frequencies (a)  $^1\text{H}$  nuclei and (b)  $^{19}\text{F}$  nuclei. The dotted line in the figures indicate the isotropic–nematic transition temperature.

reorientations of the molecules around short and long axes, translational diffusion, and orientational order (critical) fluctuations near the transition temperature ( $T_{NI}$ ). In view of the presence of substantial dipole–dipole interaction among the several protons on the molecule their hetero-nuclear coupling with the lone fluorine is neglected, and the proton data are analyzed based on homo-nuclear dipolar interactions among them [1].

### 3.1.1. Molecular reorientations

Molecular reorientations about the long axis and dynamics of end-chains are too fast of the present experiment, providing at best a constant background. Random reorientations about the short axes, characterized by the correlation time  $\tau_R$ , lead to frequency-dependent relaxation rate [3,18]

$$R_{1HR} = A_{1HR} \sum_{p=1}^2 \frac{p^2 \tau_R}{1 + (p\omega\tau_R)^2}. \quad (1)$$

Here  $A_{1HR}$  represents the coupling strength of this mechanism to the lattice modes. This contribution could also become frequency independent for experimental condition satisfy  $\omega\tau_R \ll 1$ , depending then only on  $T$ .

### 3.1.2. Critical fluctuations

Near the transition, fluctuations of the orientational order parameter manifest as slow modulations, and their characteristic time ( $\tau_{CF}$ ) increases critically as  $T_{NI}$  is approached [1,19]. This contribution is given by

$$R_{1HCF} = A_{HCF} \left[ \frac{\tau_{CF}}{1 + \sqrt{1 + \omega^2 \tau_{CF}^2}} \right]^{\frac{1}{2}}. \quad (2)$$

Here  $A_{HCF}$  is a temperature dependent parameter quantify the effective spin coupling to order fluctuations. The total proton spin-lattice relaxation rate of protons is thus expressed, including a constant background ( $R_{1H0}$ ) due to very fast processes, as

$$R_{1H} = R_{1H0} + R_{1HR} + R_{1HCF}. \quad (3)$$

### 3.2. Fluorine relaxation

The fluorine spin-lattice relaxation in the present system could be due to several mechanisms: homo-nuclear dipole interaction with fluorines present on different molecules; hetero-nuclear dipole interaction with protons; chemical shift anisotropy (CSA); and spin-rotation interaction with the molecular angular momentum components. The contribution from first interaction between the two fluorines (located on each of the molecules) is expected to be very small, and dispersionless in the present experiment. And CSA mechanism is unimportant in the present range of Larmor frequency.

It is convenient to discuss the effect of hetero-nuclear coupling between  $^1\text{H}$  and  $^{19}\text{F}$  in the high field (WC: weak-coupling limit) and low-field (SC: strong-coupling limit) regimes separately. In the former case, when the difference in the resonance frequencies of the two participating nuclear species (say  $I$  for fluorine and  $S$  for proton) is much larger than their line-widths, the dipolar perturbation leads to a coupling between the two Zeeman reservoirs. This can in principle result in a longitudinal magnetization recovery on two time scales. For the  $I$ -spin system, say, the magnetization decay to equilibrium is described by [3]

$$\frac{d\langle I_z \rangle}{dt} = -\frac{1}{T_1^I} (\langle I_z \rangle - I_0) - \frac{1}{T_1^S} (\langle S_z \rangle - S_0), \quad (4)$$

where

$$\frac{1}{T_1^I} = \gamma_I^2 \gamma_S^2 \hbar^2 S(S+1) \left\{ \frac{1}{12} J^{(0)}(\omega_I - \omega_S) + \frac{3}{2} J^{(1)}(\omega_I) + \frac{3}{4} J^{(2)}(\omega_I + \omega_S) \right\}, \quad (5a)$$

$$\frac{1}{T_1^S} = \gamma_I^2 \gamma_S^2 \hbar^2 I(I+1) \left\{ -\frac{1}{12} J^{(0)}(\omega_I - \omega_S) + \frac{3}{4} J^{(2)}(\omega_I + \omega_S) \right\}. \quad (5b)$$

$\langle I_z \rangle$ ,  $\langle I_0 \rangle$ ,  $\langle S_z \rangle$  and  $\langle S_0 \rangle$  stand for the instantaneous and equilibrium longitudinal magnetizations of the two systems, respectively. However, experimental observation of only a single time constant for recoveries of the magnetizations of both the spin systems (over three decades of time) indicates that the first term in Eq. (4) is adequate for our analysis. Thus the effect of the coupling between  $^1\text{H}$  and  $^{19}\text{F}$  manifests as a modified expression for the spin-lattice relaxation rate of fluorine Eq. (5a), unlike the case of protons. Contributions to the fluorine relaxation rate due to its dipolar coupling to protons are computed accordingly Eq. (5a), taking into account the time modulations due to short axes reorientations ( $R_{1FR}$ ) and critical fluctuations of the order parameter ( $R_{1FCF}$ ), besides including a constant background term  $R_{1F0}$ . The values of  $\tau_R$  and  $\tau_{CF}$  obtained from the proton data provide useful inputs for the fluorine analysis.

The stronger fluorine spin-rotation interaction relative to protons ( $\sim 5$  times larger [20]), seems to be crucial in providing the observed strong lattice coupling, and its contribution is sensitive to the correlation times of the molecular angular momentum components [20–23]. Contribution from SR mechanism is expressed as [22]

$$R_{1FSR} = A_{SR} T \frac{\tau_{SR}}{1 + \omega^2 \tau_{SR}^2}, \quad (6)$$

where  $A_{SR}$  quantifies the degree of fluorine coupling to the lattice, and depends on the values of the fluorine spin-rotation interaction terms. In the case of molecules constituting simple liquids,  $\tau_{SR}$  is the correlation time associated with the molecular angular momentum

fluctuations (typically in the range of  $10^{-12}$ – $10^{-13}$  s). While such time scales can at best provide a negligible constant background contribution to  $R_1$  of fluorine, the experimental data strongly suggests the presence of very slow dynamic processes, exclusively probed by the fluorine nuclei.

In this context, it may be noted that earlier line width measurements on the ESR spectra of several free radicals dissolved in liquid crystals (e.g., Freed et al. [24,25]), required for their consistent interpretation of the presence of slower processes modulating the rotational diffusion of the probe molecules. These experiments, supported by subsequent 2-D ESR methods [26,27], suggest that the free radicals not only undergo such diffusion in the presence of an orienting potential (due to mean torque), but also experience the effects of sufficiently slow fluctuations of the potential itself [26]. This necessitated dealing with the problem of diffusing molecules in the presence of a slowly relaxing local structures (SRLS). These were modeled as orienting cages undergoing slow rotational diffusion (on a time scale,  $\tau_c$ ), and the corresponding relaxation theory included these degrees of freedom as relevant random variables constituting a composite stochastic model [25]. Further, these experiments also indicated that the degree of coupling of the probes to the dynamics of the liquid crystal environment depended strongly on their size and anisotropy relative to the host molecules. With this perspective, the observed strong fluorine-lattice coupling seems to be reflective of the presence of slow torques (alluded to by the earlier ESR studies) appropriately modulating the SR interaction via molecular angular momentum. While such composite processes require in principle solving a Fokker-Planck-Kramer equation for joint probability density function of the composite Markov process, we take here a more simplistic view by accounting for the effect of such modes through a Lorentzian spectral density. We represent this contribution to  $R_1$  of fluorine as

$$R_{1FC} = A_{FC} \frac{\tau_c}{1 + \omega^2 \tau_c^2}. \quad (7)$$

Here  $A_{FC}$  is a temperature dependent parameter quantifying the strength of this mechanism. Thus, we model the observed relaxation rate in the weak-coupling limit as

$$R_{1F} = R_{1F0} + R_{1FR} + R_{1FCF} + R_{1FC}. \quad (8)$$

## 4. Analysis and discussion

The proton relaxation dispersions at three temperatures in the isotropic phase were analyzed based on Eq. (3) using the non-linear least square method [28], and the best fit data are shown in Figures 2–4 and the results are summarized in Table 1. The proton spin-lattice relaxation at 11 °C away from  $T_{NI}$  is well described by individual molecular reorientations ( $R$ ) and constant background coming from other fast processes. At  $\Delta T_{NI} = 1$  and 4 °C, the dispersions need, besides  $R$ , critical fluctuations of the orientational order (CF). The correlation times  $\tau_R$  in 4OTOLFo are small compared to 4OFTOL and 4OTOLFm. For example, away from the transition ( $\Delta T_{NI} = 11$  °C),  $\tau_R$  is 1 ns in the present system while it is 1.39 ns in 4OTOLFm [30] and 2.4 ns in 4OFTOL [29] (Figure 1). Typical correlation times of critical fluctuations  $\tau_{CF}$  in 4OTOLFo are comparable with those of 4OTOLFm (67 ns at  $\Delta T_{NI} = 11$  °C), but are short compared to 4OFTOL (363 ns at  $\Delta T_{NI} = 11$  °C). Also such critical fluctuations in the present system disappear quickly on heating in this system. The activation energy associated with the rotational diffusion is small in 4OTOLFo compared to the other two compounds (2.5, 7.5 and 20.8 kJ/mol for 4OTOLFo, 4OTOLFm and 4OFTOL, respectively). The only structural difference among these three compounds is the location of fluorine atom on the

**Table 1**  
Parameters extracted by fitting the  $^1\text{H}$  dispersions to Eq. (3) and the parameters in the table are explained in the text.

$\Delta T$ ( $^{\circ}\text{C}$ )	$R_{1\text{H}0}$ ( $\text{s}^{-1}$ )	$A_{1\text{HR}}$ ( $10^9 \text{ s}^{-2}$ )	$\tau_R$ (ns)	$A_{\text{HCF}}$ ( $10^3 \text{ s}^{-3/2}$ )	$\tau_{\text{CF}}$ (ns)
1	–	$1.24 \pm 0.11$	$0.98 \pm 0.11$	$13.35 \pm 2.16$	$49.40 \pm 7.17$
4	–	$1.52 \pm 0.1$	$0.75 \pm 0.15$	$11.62 \pm 2.79$	$34.03 \pm 6.03$
11	$0.12 \pm 0.05$	$1.85 \pm 0.04$	$1.02 \pm 0.02$	–	–

aromatic cores (see Figure 1), and further the present system is reported to be monotropic [11]. These results indicate that the activation energy for the reorientations is higher when the fluorine is located on the aromatic core nearer to the alkyl chain, and decreases considerably when it is located on the other aromatic ring. The temperature dependent data at different Larmor frequencies (shown in Figure 5a) support the predominance of CF contribution as the transition is approached from above.

Analysis of fluorine data in the WC limit based on Eq. (8), with the above values for  $\tau_R$  and  $\tau_{\text{CF}}$ , leads to the determination of  $\tau_C$  characterizing the slow torques experienced by the probe. We demonstrated clearly the necessity to include spin–rotation contribution to account for the experimental data: for 400 kHz and above (Figure 6). We find that  $\tau_C$  is in the range of 230–280 ns (Table 2), and is practically the same over the temperature range within the errors of estimation. It is interesting to note that similar time scales were obtained from the fluorine data in 4OFTOL (290 ns) [29] and 4OTOLFm (270 ns) [30] as well. The insensitivity of protons to this dynamics is understood as due to its relatively smaller spin–rotation constant.  $A_{1\text{FR}}$  and  $A_{\text{FCF}}$  (Table 2) represent the coupling strengths of the fluorine system to the lattice via the heteronuclear dipolar interaction with protons, arising from different time modulations (R and CF).

The analysis of the data in the SC limit (typically below 400 kHz in the present sample) differs from the above. We find that the extrapolated relaxation rates based on the above fit parameters deviate substantially, and systematically, from the experimental observations (Figure 6). The additional contribution in this regime arises from a qualitatively different relaxation path made available, once the fluorine and proton resonance lines start overlapping significantly. In terms of nuclear spin Hamiltonian comprising of the Zeeman term and a perturbing nuclear dipole–dipole interaction, and with the valid assumption of conservation of the total energy

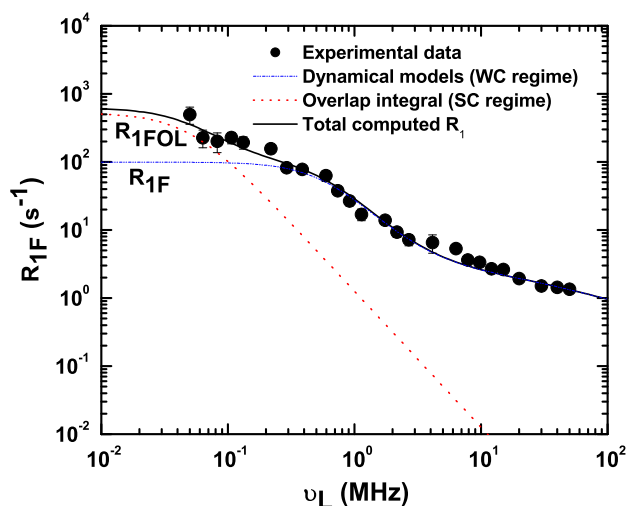


**Figure 6.** Fluorine spin–lattice relaxation rate from dynamical models and cross-relaxation (overlap integral) at  $\Delta T_{\text{NI}} = 1^{\circ}\text{C}$ .

**Table 2**  
Parameters extracted by fitting the  $^{19}\text{F}$  dispersions to Eq. (8) and the parameters in the table are explained in the text.

$\Delta T$ ( $^{\circ}\text{C}$ )	$A_{1\text{FR}}$ ( $10^9 \text{ s}^{-1}$ )	$\tau_R$ (ns)	$A_{\text{FCF}}$ ( $10^3 \text{ s}^{-3/2}$ )	$\tau_{\text{CF}}$ (ns)	$A_{\text{FC}}$ ( $10^8 \text{ s}^{-2}$ )	$\tau_C$ (ns)
1	$0.4 \pm 0.02$	1	$13.53 \pm 0.13$	49.5	$0.35 \pm 0.02$	$275.15 \pm 28.74$
4	$0.5 \pm 0.01$	1	$9.57 \pm 0.13$	34	$0.35 \pm 0.02$	$233.5 \pm 22.07$
11	$1.30 \pm 0.01$	1	–	–	$0.36 \pm 0.02$	$263.65 \pm 24.97$

of the Hamiltonian, the generalized question of spin relaxation phenomenon is connected essentially with finding out the probability of resonant absorption at a given frequency. This in turn inquires, particularly in the SC regime, into the rate at which the Zeeman and dipolar energies could come into mutual equilibrium [31]. In the presence of significant overlap of lines, the resulting transition probability for the Zeeman energy of a spin to be converted into dipolar energy leads to a characteristic time ( $T_{21}$ ), which is intermediate in nature between the spin–spin relaxation time and the spin–lattice relaxation time. This process will become rapidly ineffective if the difference in the Zeeman splittings of the two spins becomes larger than the spin–spin (dipolar) coupling among them. The simplified expression for  $T_{21}^{-1}$ , assuming specified line shapes  $g(\nu)$  for the two NMR lines (of proton and fluorine) is given by [31]

$$T_{21}^{-1} = A_{\text{OL}} \iint g_{\text{H}}(\nu') g_{\text{F}}(\nu'') \delta(\nu' - \nu'') d\nu' d\nu'' \quad (9)$$

with

$$A_{\text{OL}} = |(E_{\text{H}}, E_{\text{F}} | H_{\text{HF}}^d | E_{\text{H}} \pm h\nu, E_{\text{F}} \pm h\nu)|^2.$$

Here  $A_{\text{OL}}$  is related to the square of the matrix element of Hamiltonian involving simultaneous energy-compensating flip-flops of the two spin species mediated by appropriate terms in the dipolar interaction. To proceed further, we assume Lorentzian shapes for both the resonance lines with widths  $\Delta_{\text{H}}$  and  $\Delta_{\text{F}}$ , for proton and fluorine respectively. The resultant contribution to the fluorine relaxation rate, denoted by  $R_{1\text{FOL}} = T_{21}^{-1}$ , is clearly dependent on the extent of overlap of the two resonance lines. With this additional mechanism, we express the total computed contribution to the fluorine relaxation as a sum of the dynamic contribution  $R_{1\text{F}}$  from WC regime and cross relaxation rate  $R_{1\text{FOL}}$  with proton:

$$R_{1\text{F}}^{\text{T}} = R_{1\text{F}} + R_{1\text{FOL}}.$$

We now account for the differential contribution in the SC regime (Figure 6),  $(R_{1\text{EXPT}} - R_{1\text{F}})$ , as arising from  $R_{1\text{FOL}}$ , and fit the corresponding data to Eq. (9) to obtain the three variable parameters ( $A_{\text{OL}}$ ,  $\Delta_{\text{H}}$  and  $\Delta_{\text{F}}$ ). In Figure 6, we also include  $R_{1\text{FOL}}$ , along with contributions from dynamic models ( $R_{1\text{F}}$ ) from Eq. (8) to compare the total computed relaxation rate with the experimental data. In view of the limited number of data points pertaining to this region of overlap (due to instrument limitations) the data fit to  $R_{1\text{FOL}}$  in terms of Eq. (9) is to be viewed more as an interesting demonstration of this mechanism that could be detected in the FCNMR experiment, and the values of the fit parameters are thus seen as providing reasonable order-of-magnitude estimates. We observe that the width of the Lorentzian line of the protons is about 4 kHz while that of the fluorine is about 40 kHz. It may be further pointed out that the line widths obtained here are intrinsic and are free from the instrument artifacts, since the observations pertain to dipolar interactions between nuclei residing on the same molecule. The larger fluorine line width is consistent with our interpretation of the SC regime relaxation data based on much slower local modes: they contribute more to the spectral density  $J^{(0)}$  as probed by fluorine, and hence to its line width. While the fluorine relaxation is seen

to be profoundly influenced in the SC regime by  $T_{21}$  process, such is not the case with protons. There are several protons residing on the molecule having homo-nuclear dipolar interaction all through the dispersion regime (and thus having appreciable overlap integral values always), and addition of one more such coupling with fluorine at the onset of the SC regime is obviously not making an observable difference.

Figure 5b shows the temperature dependent spin–lattice relaxation data of fluorine at different Larmor frequencies. At 10 MHz the relaxation rate is independent of temperature, and at 1 and 0.2 MHz it shows two maxima within the temperature range of our study. These maxima in the low frequency data seems to betray the presence of possibly several slow processes in the system, but their quantitative interpretation however is difficult, complicated by the additional cross-relaxation process triggered in this frequency range.

## 5. Conclusions

In this Letter we presented results of our measurements of proton and fluorine spin–lattice relaxation rates in the isotropic phase of a liquid crystal 4OTOLFO. We find that the major contribution to the fluorine relaxation arises from spin–rotation interaction, while proton relaxation could be accounted from the known dipolar relaxation pathways. Proton dispersions provide an insight into the individual reorientational dynamics and collective order parameter fluctuations near the isotropic-nematic phase transition. The fluorine dispersion profiles, showing strong coupling to the lattice and strong dispersion extending to very low frequencies, required invoking of other slower processes, as has been already suggested by earlier ESR studies. This is traced to the presence of slowly relaxing local structures, coupling to the fluorine system rather exclusively through spin–rotation interaction. We also observed that at low enough frequencies the dipolar interaction between proton and fluorine transits from weak to strong coupling limit, and acquires a degree of homo-nuclear character. This in turn provides an additional relaxation path to fluorine via cross-relaxation. Protons are not particularly sensitive in reporting on this mechanism in our experiment because of their abundant homo-nuclear dipolar coupling within the molecule. The present FCNMR experiment demonstrated clearly the effects of level crossing between the two spin systems through low frequency enhancement of the lattice coupling of the rare spin species ( $^{19}\text{F}$ ). The differing temperature dependences of the relaxation rates also point to the

presence of qualitatively different pathways to the spin–lattice relaxation of the two spin systems.

## References

- [1] R.Y. Dong, Nuclear Magnetic Resonance of Liquid Crystals, Springer Verlag, 1997.
- [2] R.Y. Dong, Nuclear Magnetic Resonance spectroscopy of Liquid Crystals, World Scientific Publishing Co., 2010.
- [3] A. Abragam, The Principles of Nuclear Magnetism, Clarendon Press, Oxford, 1961.
- [4] R.Y. Dong, Prog. Nucl. Magn. Reson. Spectrosc. 41 (2002) 115.
- [5] R.Y. Dong, Annu. Rep. NMR Spectrosc. 53 (2004) 68.
- [6] C. Catanescu, L.C. Chien, S.T. Wu, Mol. Cryst. Liquid Cryst. 411 (2007) 93.
- [7] Y.M. Liao, N. Janarthan, C.S. Hsu, S. Gauza, S.T. Wu, Liquid Cryst. 33 (2006) 1199.
- [8] S. Gauza, S.T. Wu, A. Spadlo, R. Dabrowski, J. Display Technol. 2 (2006) 247.
- [9] S. Gauza, C. Wen, Y. Zhao, S.T. Wu, A. Ziolek, R. Dabrowski, Mol. Cryst. Liquid Cryst. 453 (2006) 215.
- [10] S. Gauza, J. Li, S.T. Wu, A. Spadlo, R. Dabrowski, Y. Tzeng, K. Cheng, Liquid Cryst. 32 (2005) 1077.
- [11] J. Czub, S. Urban, R. Dabrowski, B. Gestblom, Acta Phys. Pol. A 107 (2005) 947.
- [12] J. Li, S. Gauza, S.T. Wu, Opt. Express 12 (2004) 2002.
- [13] D. Demus, Y. Goto, S. Sawada, E. Nakagawa, H. Saito, R. Tarana, Mol. Cryst. Liquid Cryst. 260 (1995) 1.
- [14] Il-Kook Huh, Yong-Bae Kim, Liquid Cryst. 29 (2002) 1265.
- [15] A. Spadlo et al., Liquid Cryst. 30 (2003) 191.
- [16] A. Spadlo, J. Dziaduszek, R. Dabrowski, K. Czuprynski, S.T. Wu, SPIE 4759 (2002) 79.
- [17] R. Kimmich, E. Anardo, Prog. Nucl. Magn. Reson. Spectrosc. 44 (2004) 257.
- [18] N. Bloembergen, E.M. Purcell, R.V. Pound, Phys. Rev. 73 (1948) 679.
- [19] F.V. Chavez, F. Bonetto, D.J. Pusiol, Chem. Phys. Lett. 330 (2000) 368.
- [20] H.S. Gutowsky, I.J. Lawrenson, K. Shimomura, Phys. Rev. Lett. 6 (1961) 349.
- [21] P.S. Hubbard, Phys. Rev. 131 (1963) 1155.
- [22] D.K. Green, J.G. Powles, Proc. Phys. Soc. 85 (1965) 87.
- [23] R.J.C. Brown, H.S. Gutowsky, K. Shimomura, J. Chem. Phys. 38 (1963) 76.
- [24] J.H. Freed, J. Chem. Phys. 66 (1977) 4183.
- [25] J.H. Freed, A. Nayeem, S.B. Rananavare, in: G.R. Luckhurst, C.A. Veracini (Eds.), The Molecular Dynamics of Liquid Crystals, Kluwer, 1994. (Chap. 4); J.H. Freed, A. Nayeem, and S.B. Rananavare, in: G.R. Luckhurst, C.A. Veracini (Eds.), The Molecular Dynamics of Liquid Crystals, Kluwer, 1994 (Chap. 5 and references therein).
- [26] V.S.S. Sastry, A. Polimeno, R.H. Crepeau, J.H. Freed, J. Chem. Phys. 105 (1996) 5753.
- [27] V.S.S. Sastry, A. Polimeno, R.H. Crepeau, J.H. Freed, J. Chem. Phys. 105 (1996) 5773.
- [28] W.H. Press, B.P. Flannery, S.A. Teukolsky, W.T. Vetterling, Numerical Recipes, The Art of Scientific Computation, Cambridge University Press, Cambridge, 1986.
- [29] M. Rajeswari, Trivikram R. Molugu, Surajit Dhara, K. Venu, V.S.S. Sastry, R. Dabrowski, J. Chem. Phys. 135 (2011) 244507.
- [30] M. Trivikram Rao, M. Rajeswari, K. Venu, V.S.S. Sastry, R. Dabrowski, Phys. Rev. E., submitted for publication.
- [31] N. Bloembergen, S. Shapiro, P.S. Pershan, J.O. Artman, Phys. Rev. 114 (1959) 445.